Bleed Interactions in Supersonic Flow

A. Hamed[1] , S. Manavasi[2] , D. Shin[2], A. Morell[2] and C. Nelson[3]
[1,2] School of Aerospace Systems,
University of Cincinnati, Cincinnati, Ohio 45221
[3] Innovative Technology Applications, Chesterfield, Missouri 63006

[Received date; Accepted date] – to be inserted later

ABSTRACT

A parametric study is conducted to characterize the flow throughout supersonic flow bleed regions and to investigate the effects of free stream Reynolds number and incoming boundary layer thickness. Numerical solutions of the compressible Navier-Stokes equations are obtained in a domain that includes the passages within a bleed-hole row and plenum in addition to the external flow. A turbulence model based on the two-equation SST model is employed to enable the resolution of large separated flow regions inside the normal bleed holes. Computational results are presented to show the effects of free stream Reynolds number on the external flow above and downstream of the bleed region. Stagnation pressure contours are compared at various stream-wise locations for different incoming boundary layer thicknesses as well. The results show that the freestream Reynolds number has a strong influence on the total pressure distortion and on the secondary flow in the cross sectional planes downstream of the bleed region.

1. INTRODUCTION

Holes, slots, and scoops have been used in mixed compression supersonic inlet systems to control the boundary layer and improve supersonic inlet stability and pressure recovery. Because of their higher pressure recovery slanted bleed angles are used in the forward inlet regions to reduce the momentum drag of overboard bleed flow. On the other hand, normal bleed is needed in the throat region for maximum terminal shock stability. The closer to the throat the terminal shock is allowed, the higher the inlet recovery. However along with this benefit comes the increased risk of unstarting the inlet. The dynamics of inlet and engine compression systems are coupled, since unstart can result in compressor surge/stall and vice versa [1]. Hence these unsteady flow events could occur individually or in combination, where one precipitates the other. The uncontrolled release of energy by these events can trigger fairly violent aerodynamic responses, including momentary or permanent performance loss of engine operation and catastrophic physical damage of the engine structure. Preventing boundary layer separation [2] and controlling its growth in shock wave interaction regions through bleed [3] is necessary, but must be achieved with minimum loss in performance.

Supersonic inlet bleed is often accomplished through bands of tightly spaced bleed-hole rows located in adverse pressure gradient regions caused by shock wave/boundary layer interactions. Bleed models that simulate the effects of mass removal are required in mixed supersonic inlet design and analysis, since it is impractical to resolve the flow field through each of the individual holes in these bands. The models, when implemented as a boundary condition in simulations that only resolve the flow outside the bleed surface should predict not only the mass flux through the bleed regions but also relate the associated changes in the external flow and boundary layer to the bleed configuration and local free stream conditions. However, with few exceptions [4-5] bleed models have consisted mainly of empirical correlations of mass flux. Abrahamson [6] and Dambara et.al [7] derived their bleed models based on isentropic nozzle flow equations. Harloff and Smith [8] derived generalized sonic flow coefficient correlations based on Bragg's orifice flow model [9] which they validated through comparisons with comprehensive experimental data sets. The data included single, multiple, normal, slanted, subsonic, transonic and supersonic bleed through round holes as well as normal slots. The comparisons indicated that the agreement between their model predictions and the experimental data

[1] Bradley Jones Professor, School of Aerospace Systems
[2] Graduate student, School of Aerospace Systems
[3] Senior Scientist

was close for subsonic and supersonic flow cases but not for transonic 1.27 free stream Mach number.

Computational results obtained using these bleed models [10] in shock wave/turbulent boundary-layer interactions under-predicted the maximum static pressure downstream of the interactions compared to the experimental data of Willis et.al [11] which led to discrepancies in the computed bleed mass flow. Similarly, Dambara et.al [7] attributed the differences between their computational results and the experimental measurements of Hingst and Tanji [12] and Benhachami and Berger [13] to discrepancies in the computed bleed mass flux. Hamed et.al [14] also reported differences between the numerical predictions of external Mach number above the bleed surface and the bleed mass flow through each of the six rows of staggered normal bleed holes using bleed models and those obtained from three dimensional simulations which resolved the flow within the bleed-hole passages. Slater [15] reported differences among the mass flux predictions by three bleed models in the WIND-US code through an oblique shock-wave/boundary-layer interaction configuration derived from a "parameterized" supersonic inlet. The differences between the bleed model predictions were noticeable upstream of the oblique shock where some models did not bleed any flow while others predicted negative bleed (injection) even though the model coefficients were adjusted to provide the same overall bleed. Akatsuka et.al [16] and Slater [17] subsequently proposed modifications to improve predictions at high bleed pressure ratios and to allow blowing into the main stream.

Other computational studies that resolved the flow within the bleed passages [18-23] considered different bleed configurations including normal, slanted, single and multiple bleed holes and slots and reported the effects of bleed configuration and its position relative to the impinging shock on both external and bleed flow in the interaction region. These studies revealed interesting flow features in the bleed region and within the bleed passages including local shocks that form across each bleed opening, which were reported first by Hamed and Lehnig [24] and later by Hamed et.al [25] and by Rimlinger et.al [26] who coined the term "barrier shock". The pressure gradient created by these local shocks could be higher than that created by the impinging shock since they form after the flow goes through Prandtl-Meyer expansion into the bleed cavity. Davis et.al [27] presented detailed experimental measurements within normal bleed slots that compared very closely with the computational results of Hamed et.al [28] in the same bleed configuration. The agreement between the two studies lends confidence to the numerical predictions of the complex flow field inside and outside the bleed passages and its influence on the external flow.

Hamed et.al [14] compared the numerical predictions of external flow above and behind a six rows of staggered normal bleed holes using bleed models and those obtained from three dimensional simulations which resolved the flow within the bleed-hole passages. Figure 1 presents the computed

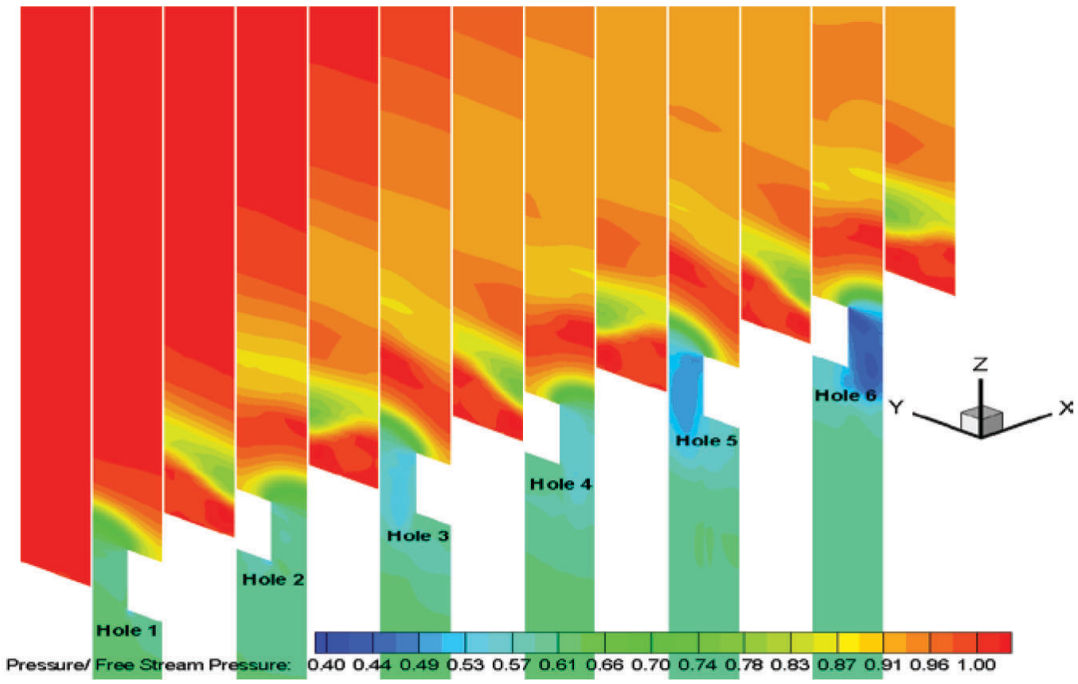

Figure 1: Static pressure contours in cross-sectional planes for multiple hole case (M = 1.27, Re = 1.426 × 10^7/m)

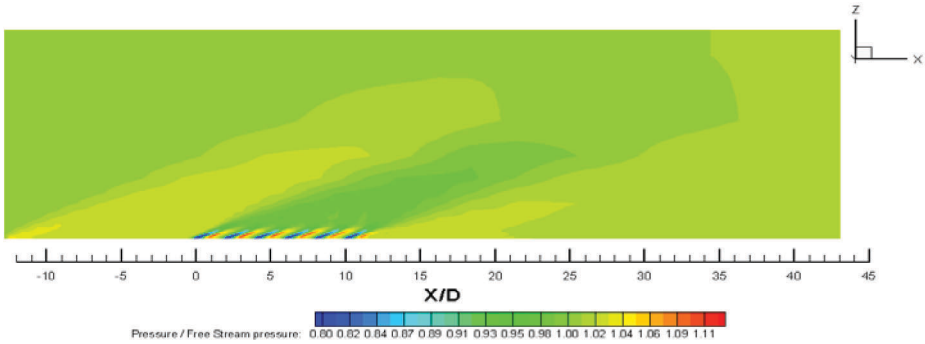

Figure 2a: Static pressure contours for resolved bleed multiple hole case (M = 1.27, Re = 1.426 × 10^7/m)

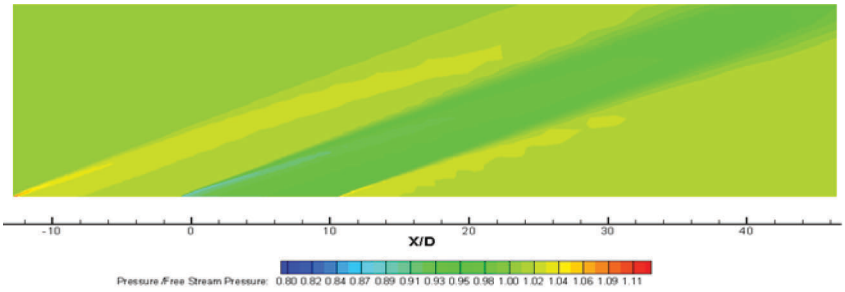

Figure 2b: Static pressure contours for multiple hole case with bleed boundary condition (M = 1.27, Re = 1.426 × 10^7/m)

Mach number contours by Hamed et.al [14] at different axial locations through the six rows of bleed holes. This figure demonstrates the cascading of expansion and compression waves that are generated at each of the bleed holes. This phenomenon could not be predicted by the simulations that used bleed boundary conditions and only resolved the flow field above the bleed surface as can be concluded from a comparison of Figure 2a and b. The bleed model is seen to produce a strong localized expansion at the start of the bleed zone and a strong shock at the end, that are unlike the alternating expansion compression wave pattern seen in the computations that resolved flow through bleed passage. No experimental or numerical supersonic bleed studies have considered the effect of free stream Reynolds number in spite of experimental evidence that it strongly influences flow separation [2].This paper presents results from numerical simulations conducted to investigate the three-dimensional flow characteristics associated with bleed through multiple holes in supersonic flow. Numerical solutions to the compressible Navier-Stokes equations were obtained in a domain that includes the plenum and the passages inside the bleed holes in addition to the external flow. Results are presented for the external flow development at various locations downstream of bleed indicate bleed generated pressure waves that propagate into the external flow and the formation of a complex three-dimensional flow near the bleed surface. Each bleed hole in the row induced either two or four counter-rotating vortices that distorted the stagnation pressure contours. The external flow interactions are compared for different free stream Reynolds numbers and incoming boundary layer thicknesses.

2. BLEED CONFIGURATION AND COMPUTATIONAL DETAILS

The bleed geometry consisted of a single row of 6.35 mm diameter, 90 degree round holes with a lateral distance of 2D between the centers of neighboring holes, and a length to diameter ratio, L/D, of one. These parameters correspond to one of the configurations used in the experimental investigation of Willis et al. [29]. Figure 3 depicts the computational domain employed in the flows simulations with X,Y,Z = 0 at the bleed surface hole center. The solution domain extended 50D above the bleed surface and 50D downstream of the bleed-hole row, to minimize the upper solution domain boundary interactions with the bleed flow, and to study the effect of bleed on the development of the external flow downstream of bleed respectively. The solution domain's width extended 1D from the center of the bleed hole to the central plane between two neighboring holes to take advantage of symmetry, and the inlet plane was located at X/D = -5. All flow variables at the downstream supersonic free-stream

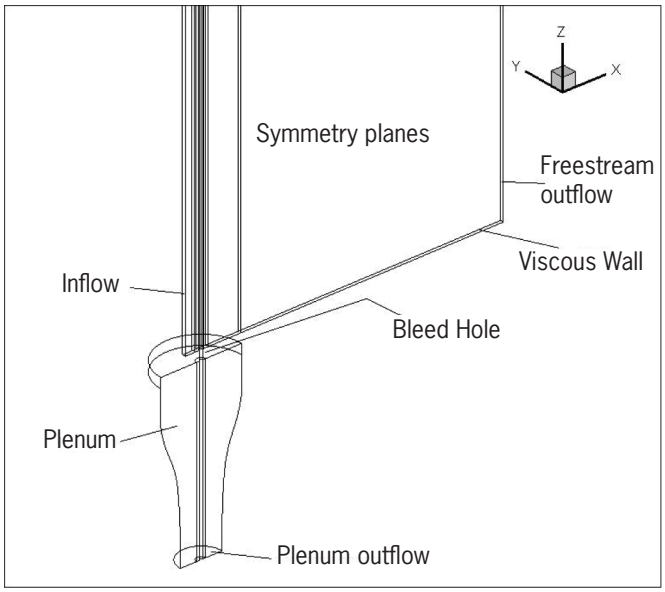

Figure 3: Schematic of computational domain with BCs

boundary were extrapolated from the interior and the static pressure was maintained sufficiently low at the plenum exit to sustain choked flow in all cases. The plenum was of a cylindrical cross-section with diameter = 10D and height = 10D.

The solution domain was discredited using a combination of O and H grids, and included a total of 2,518,808 grid points in 20 sub-domains. Referring to Figure 4, the number of grid points within the bleed hole and plenum were 634,654 and 941,391 respectively. The minimum grid spacing was 3.05×10^{-7} m in the turbulent boundary layers above the bleed surface and 3.99×10^{-6} m within the bleed hole. This ensured a maximum y+ of 1.88 for all cases.

Numerical simulations for the compressible turbulent supersonic flow were conducted using WIND-US code [30] developed and supported by the NPARC (National Program for Applications-Oriented Research in CFD), which is an alliance of NASA Glenn Research Center, U.S. Air Force Arnold Engineering Development Center, and the Boeing Company. The two-equation SST turbulence model was employed based on prior experience in simulating complex supersonic flow fields involving flow separation [31-33]. In solving the compressible Navier-Stokes equations, the 2nd order upwind HLLC scheme was used for the spatial derivative with a single stage Euler implicit local time stepping scheme. A point Jacobi implicit operator was used for the left hand side of the N-S equations with a relaxation

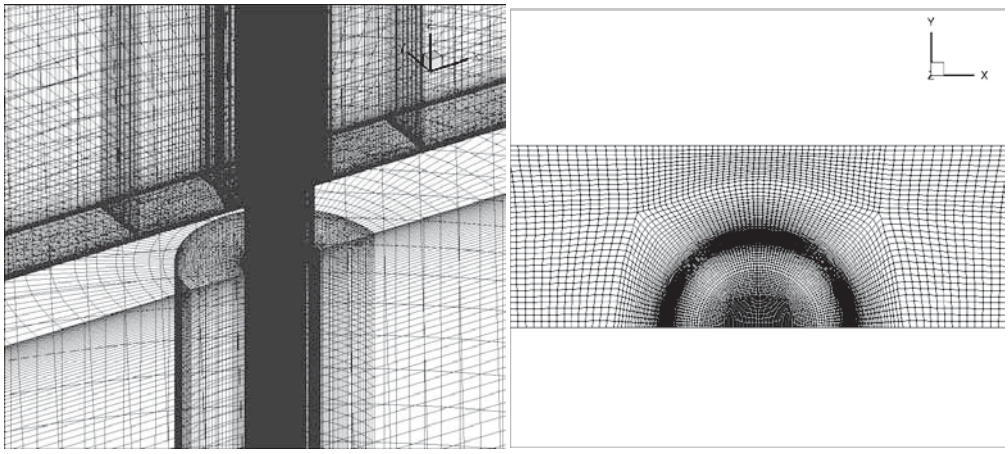

(a) Isometric view (b) View in negative Z direction

Figure 4: Computational grid in bleed region

factor of 0.75. The simulations were initialized with supersonic free-stream external flow conditions above the bleed surface and with a very low total pressure and Mach number within the holes and plenum. The initial CFL number was 0.5. It was gradually increased up to 5 as convergence was approached, for a criterion set at 10^{-8}. The effect of incoming boundary layer upstream of bleed was examined for two different boundary layer thicknesses, δ. Flow solutions for supersonic flow over a flat plate were used to provide the initial profiles at the required δ/D. FPRO, an auxiliary utility with WIND-US, was used to extract the required profiles from the flat plate solutions and initialize the bleed solutions with them. All numerical simulations used WIND-US parallel processing capability.

3. RESULTS AND DISCUSSIONS

In all simulations presented here, the freestream Mach number was 1.27. The freestream Reynolds numbers investigated were 1.138 million and 27.385 million per meter corresponding to a stagnation temperature of 292.4 K and stagnation pressures of 7.17 and 172.1 kPa, respectively. For each Reynolds number, results are presented for incoming turbulent boundary layer thicknesses of δ/D = 1.0 and 0.5.

Sample Mach contours and streamlines through a bleed hole symmetry plane are shown in Figure 5. The flow is characterized by an expansion wave into the hole and a bow bleed shock that crosses the hole opening. Within the bleed hole, the flow forms a jet adjacent to the back wall. Figure 6 presents the computed stream-wise velocity profiles at the downstream edge of a bleed hole along the two lateral symmetry planes at Y/D = 0 through the bleed-hole center line, and at Y/D =1 mid way between two neighboring holes. One can see velocities higher than the freestream value caused by the supersonic flow expansion into the bleed hole. The lower velocity near the surface at Y/D = 0 is attributed to the bow shockwave seen in Figure 5. Also included in the figure is the reference velocity profile at the inlet to the solution domain for comparison.

The corresponding static pressure contours presented in Figures 7-8 show the bleed generated expansion and shock waves above and on the bleed surface. The Reynolds number influence can be seen in the pressure contours' footprint on the bleed surface where the pressure waves extend laterally between neighboring holes at the higher Re. The wave propagation into the freestream is similar to the pattern previously predicted in multiple bleed rows (Figure 1).

Figures 9 through 12 present the stagnation pressure contours, normalized by the freestream value, at various locations downstream of the bleed-hole row with superimposed secondary flow streamlines. Only one pair of counter-rotating vortices are seen to form behind each hole in the case of Re= 1.138x106/m and d/D = 1 (Figure 9). This is similar to the experimental observations of in the case of a single bleed hole in subsonic flow (M=0.6) at a Reynolds number of 4.66x106 /m by Schoenenberger et al. [34]. However, Figures 10 through 12 indicate that an additional pair of secondary counter-rotating vortices form above the primary vortices in all other cases. The less pronounced secondary

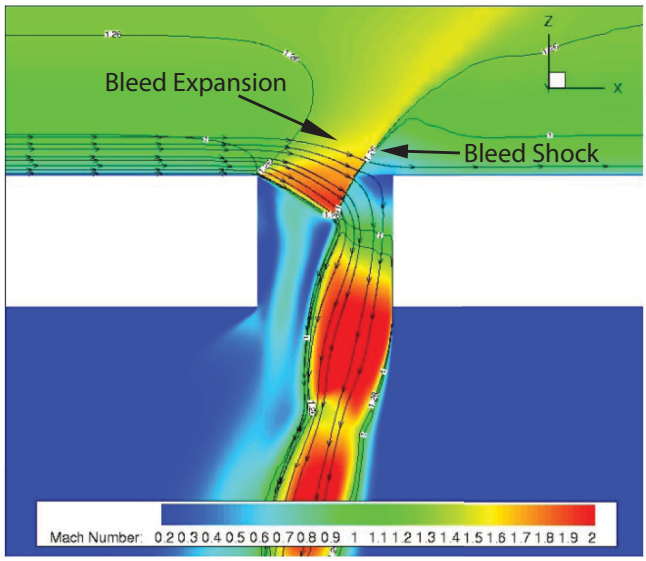

Figure 5: Mach number contours through the bleed hole central plane (M_∞ = 1.27, Re = 2.739 × 10^7/m, δ/D = 1)

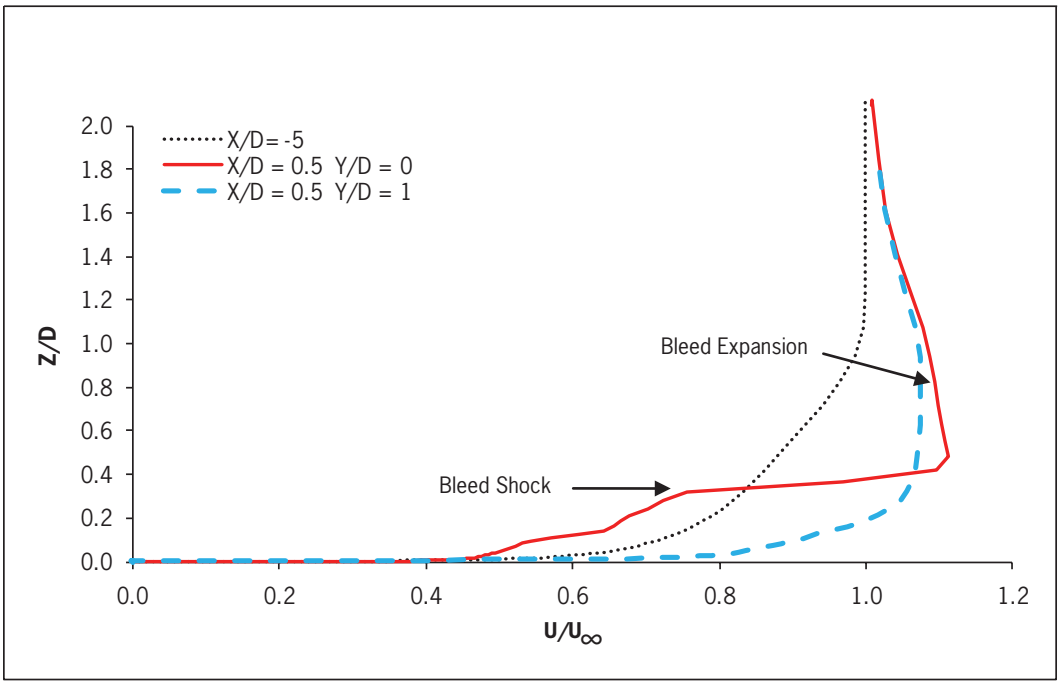

Figure 6: Stream-wise velocity profiles upstream and behind the bleed hole (M_∞ = 1.27, Re = 2.739 × 10^7/m, δ/D = 1)

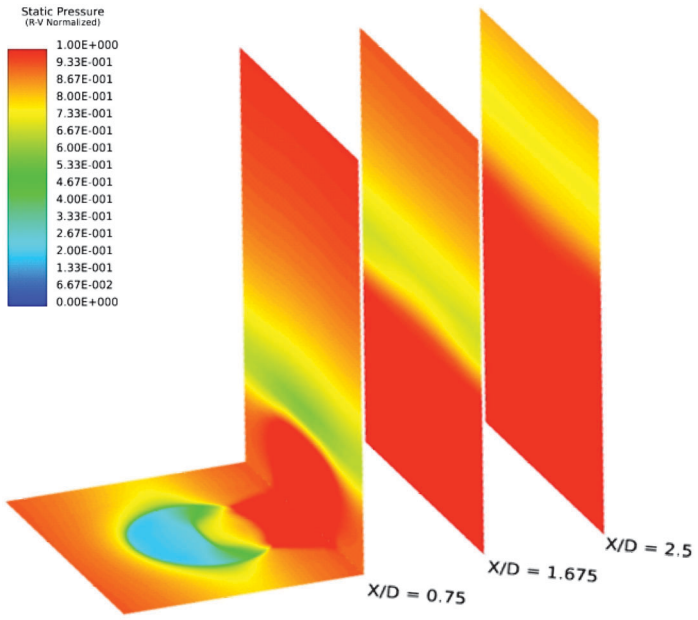

Figure 7: Static pressure contours (M = 1.27, Re = 1.138 × 10^6/m, δ/D = 1.0)

vortices dissipate before the primary vortices in the case of low Reynolds number and _/D = 0.5 (Figure 11). On the other hand, the primary vortices fold into the secondary vortices which persist further downstream in the high Reynolds number cases (Figures 10 and 12). One would conclude that, overall, more stagnation pressure distortion occurs for the thinner boundary layer; and for that case it appears that the distortion is less for the higher Reynolds number investigated.

Table 1 lists the computed maximum stream-wise vorticity (wx max) and circulation (G) magnitudes for the primary vortices. The circulation was calculated from the integration of the stream-wise vorticity over the area in which it was at least 1% of the maximum value at X/D = 2.5. The lower

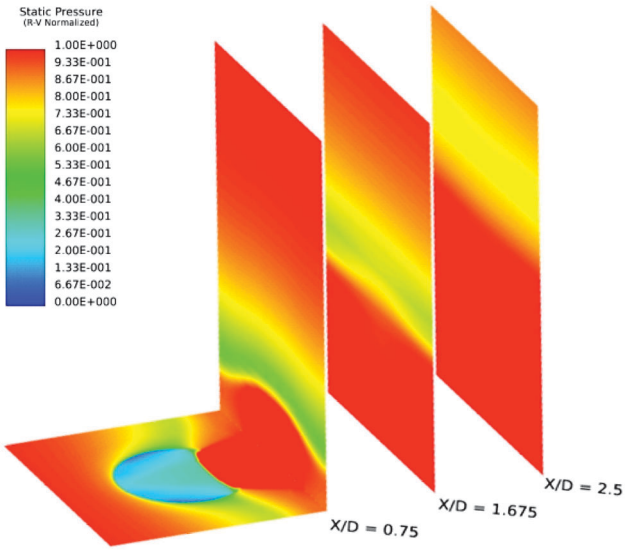

Figure 8: Static pressure contours (M = 1.27, Re = 2.739 $\times$ 10^7/m, δ/D = 1)

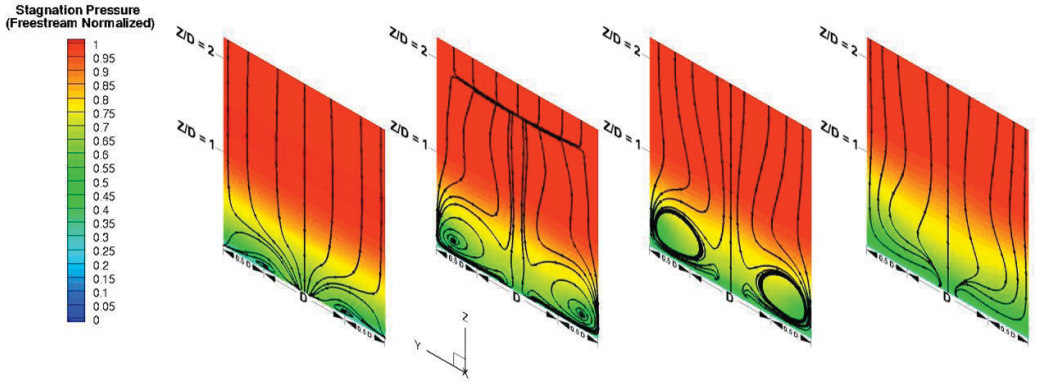

(a) X/D = 0.5 (b) X/D = 2.5 (c) X/D = 5 (d) X/D = 20

Figure 9: Total pressure contours and secondary flow (M = 1.27, Re = 1.138 $\times$ 10^6/m, δ/D = 1.0)

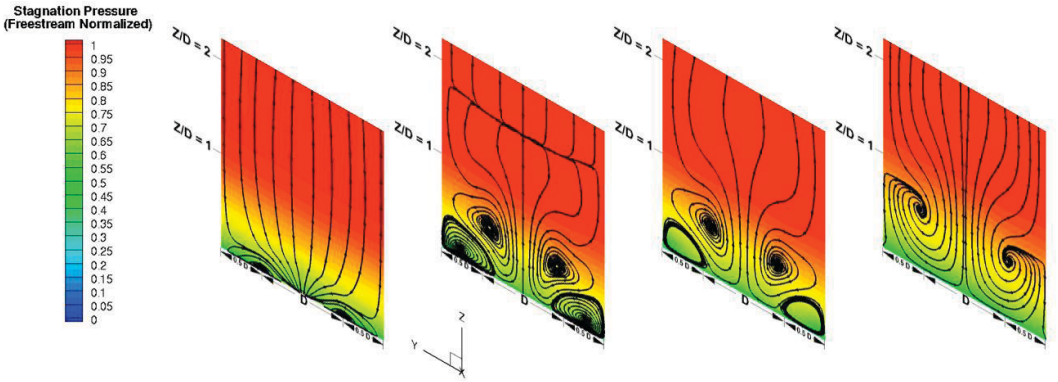

(a) X/D = 0.5 (b) X/D = 2.5 (c) X/D = 5 (d) X/D = 20

Figure 10: Total pressure contours and secondary flow (M = 1.27, Re = 2.739 $\times$ 10^7/m, δ/D = 1.0)

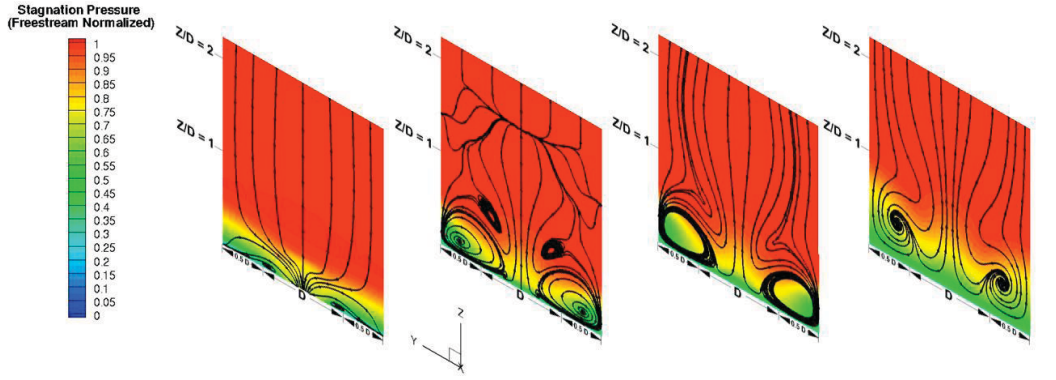

(a) X/D = 0.5 (b) X/D = 2.5 (c) X/D = 5 (d) X/D = 20

Figure 11: Total pressure contours and secondary flow (M = 1.27, Re = 1.138 × 10^6/m, δ/D = 0.5)

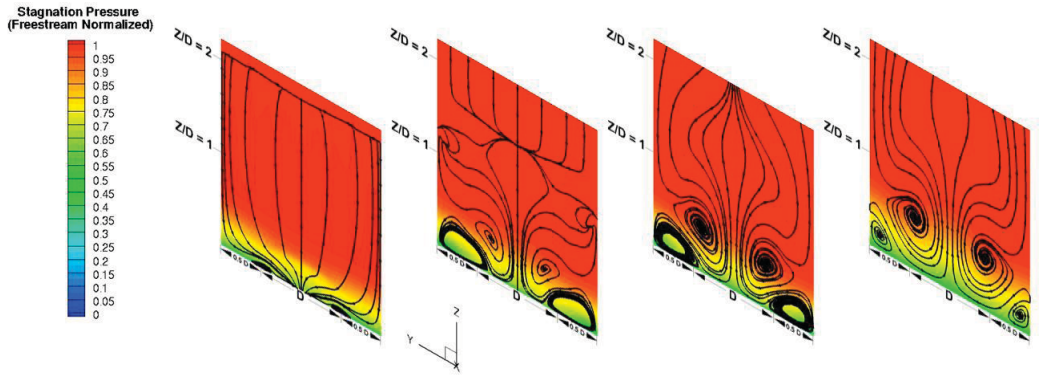

(a) X/D = 0.5 (b) X/D = 2.5 (c) X/D = 5 (d) X/D = 20

Figure 12: Total pressure contours and secondary flow (M = 1.27, Re = 2.739 × 10^7/m, δ/D = 0.5)

Reynolds number cases are seen to have higher values of circulation and maximum stream-wise vorticity than the higher Reynolds number cases at all locations. The thinner boundary layer cases have higher values of circulation and maximum stream-wise vorticity for both Reynolds numbers.

It is traditional to use the non-dimensional sonic flow coefficient (Q_{sonic}) that normalizes the actual bleed mass flow rate by the maximum theoretical value corresponding to sonic flow through the hole.

$$Q_{sonic} = \frac{W_{bleed}}{W_{sonic}} \tag{1}$$

Table 1. Circulation and maximum stream-wise vorticity of primary vortex

Re	δ/D	X/D	Γ (m^2/s)	$\omega_{x\ max}$ (1/s)
1.138 × 10^6 /m	0.5	2.5	0.149	82374
		5	0.0779	24290
	1	2.5	0.117	59411
		5	0.0530	15054
2.739 × 10^7 /m	0.5	2.5	0.0573	49760
		5	0.0245	11340
	1	2.5	0.0530	47735
		5	0.0203	10428

W_{sonic} is defined as follows:

$$W_{sonic} = pt\,A\left(\frac{\gamma g}{RT_t}\right)^{1/2}\left(1+\frac{\gamma-1}{2}\right)^{\frac{-(\gamma+1)}{2(\gamma-1)}} \quad (2)$$

where pt and T_t are the freestream stagnation pressure and temperature, A is the bleed area, R is the ideal gas constant, and g is the acceleration due to gravity. The computed sonic flow coefficient and the percentage of the incoming boundary layer mass bled are listed in Table 2 for the four cases. The results indicate that Q_{sonic} is not sensitive to Reynolds number or boundary layer thickness.

Table 2. Sonic flow coefficient and % of boundary layer mass bled

Re	1.138×10^6 m		2.739×10^7 m	
δ/D	0.5	1	0.5	1
Q_{sonic}	0.194	0.199	0.193	0.191
BL mass bled	23.7%	10.1 %	21.1 %	8.9 %

CONCLUSION

Numerical simulations were conducted to characterize the effect of bleed though a row of normal round holes in the turbulent boundary layer of supersonic flow. The three dimensional computational results indicate that the free stream Reynolds number has great influence on the stagnation pressure distortion and secondary flow behind the bleed. The distortion was greater at low Reynolds number and the associated secondary flow more complex at the high Reynolds number. The incoming turbulent boundary layer thickness was also found to influence the same parameters. However both Reynolds number and incoming boundary layer thickness did not have a significant effect on the sonic flow coefficient Q_{sonic}.

ACKNOWLEDGEMENTS

This work was sponsored by NASA Glenn Research Center Cooperative Agreement NNX07AC69A, Dr. John Slater project monitor. The authors would like to acknowledge the invaluable technical support of Mr. Rob Ogden, University of Cincinnati Department of Aerospace Engineering and Engineering Mechanics.

REFERENCES

[1] K. Numbers and A. Hamed, Conservation Coupling Techniques for Dynamic Inlet-Engine Analysis, *Journal of Propulsion and Power*, Vol. 19, No. 3, May-June 2003, pp. 444-455

[2] A. Hamed and A. Kumar, Flow Separation in Shock Wave Boundary Layer interactions, *Journal of Engineering for Gas Turbines and Power*, Vol. 116, January, 1994, pp. 98-103.

[3] A. Hamed and J. S. Shang, Survey of Validation Data Base for Shock Wave Boundary Layer Interactions in Supersonic Inlets, *J. of Propulsion*, Vol. 7, No. 4, July-Aug. 1991, pp. 617-6258.

[4] J. Lee, M. L. Sloan and G. C. Paynter, Lag Model for Turbulent Boundary Layers over Rough Bleed Surfaces, *Journal of Propulsion and Power*, Vol. 10, No.4, July-August 1994, pp. 562-568.

[5] J. Lee and G. C. Paynter, Modified Spalart-Allmaras One-Equation Turbulence Model for Rough Wall Boundary Layers, *J. of Propulsion*, Vol. 12, No. 4, 1996, pp. 809-812.

[6] K. W. Abrahamson, *Numerical Investigation of a Mach 3.5 Axisymmetric Inlet with Multiple Bleed Zones*, AIAA Paper 1988, 2588.

[7] S. Dambara, M. Yamamoto and S. Honami, *Modeling of Boundary Condition for Turbulent Boundary Layer Bleed*, AIAA Paper 1998, 0926.

[8] G. J. Harloff and G. E. Smith, Supersonic-Inlet Boundary-Layer Bleed Flow, *AIAA Journal*, Vol. 34, No. 4, April 1996, pp. 778-785.

[9] S. L. Bragg, Effect of Compressibility on the Discharge Coefficient of Orifices and Convergent Nozzles, *Journal of Mechanical Engineering Science*, Vol. 2, No. 1, 1960, pp. 35-44.

[10] G. J. Harloff and G. E. Smith, *Numerical Simulation of Supersonic Flow Using a New Analytical Bleed Boundary Condition*, AIAA Paper 1995, 2759.

[11] B. Willis, D. Davis and W. Hingst, *Flowfield Measurements in a Normal-Hole-Bled Oblique Shock Wave and Turbulent Boundary Layer Interaction*, AIAA Paper 1995, 2885.

[12] W. R. Hingst and F. T. Tanji, *Experimental Investigation of a Two-Dimensional Shock-Turbulent Boundary Layer Interaction with Bleed*, AIAA Paper 1983, 0135.

[13] D. Benhachmi, I. Greber and W. Hingst, *Experimental and Numerical Investigation of an Oblique Shock Wave/Turbulent Boundary Layer Interaction with Continuous Suction*, AIAA Paper 1989, 0357.

[14] A. Hamed, Z. Li, S. Manavasi and C. Nelson, *Flow Characteristics through porous bleed in supersonic turbulent boundary layers*, AIAA Paper 2009, 1260.

[15] J. W. Slater, *Verification Assessment of Flow Boundary Conditions for CFD Analysis of Supersonic Inlet Flows*, AIAA Paper 2001, 3882.

[16] J. Akatsuka, Y. Watanabe, A. Murakami and S. Honami, *Porous Bleed Model for Boundary Condition of CFD Analysis*, AIAA Paper 2006, 3682.

[17] J. W. Slater, *Improvements in Modeling 90 Degree Bleed Holes for Supersonic Inlets*, AIAA Paper 2009, 0710.

[18] A. Hamed and Z. Li, *Simulation of Bleed-Hole Rows for Supersonic Turbulent Boundary Layer Control*, AIAA Paper 2008, 67.

[19] A. Hamed, J. J. Yeuan, and S. H. Shih, Shock-Wave Boundary Layer Interactions with Bleed, Part 1: Effect of Slot Angle, *Journal of Propulsion and Power*, Vol. 11, No. 6, November-December 1995, pp. 1231-1235.

[20] A. Hamed, J. J. Yeuan, and S. H. Shih, Shock-Wave Boundary Layer Interactions with Bleed, Part 2: Effect of Slot Location, *Journal of Propulsion and Power*, Vol. 11, No. 6, November-December 1995, pp. 1236-1241.

[21] T. I-P. Shih, Control of Shock-Wave/Boundary-Layer Interactions by Bleed, *International Journal of Fluid Machinery and Systems*, Vol. 1, No. 1, October-December 2008, pp. 24-32.

[22] A. J. Flores, T. I-P Shih, D. O. Davis and B. P. Willis, *Bleed of Supersonic Boundary-Layer Flow Through Rows of Normal and Inclined Holes*, AIAA Paper 1999, 2112.

[23] Y. L. Lin, M. A. Stephens, T. I-P Shih and B. P. Willis, *Effects of Plenum Size on Bleeding a Supersonic Boundary Layer*, AIAA Paper 1997, 0609.

[24] A. Hamed and T. Lehnig, Investigation of Oblique Shock/Boundary-Layer Bleed Interaction, *Journal of Propulsion and Power*, Vol. 8, No. 2, March-April 1992, pp. 418-424.

[25] A. Hamed, S. H. Shih and J. J. Yeuan, *An Investigation of Shock/Turbulent Boundary Layer/Bleed Interaction*, AIAA Paper 1992, 3085.

[26] M. J. Rimlinger, T. I-P. Shih and W. J. Chyu, *Three-Dimenensional Shock-Wave/Boundary-Layer Interactions with Bleed Through a Circular Hole*, AIAA Paper 1992, 3084.

[27] D. O. Davis, B. P. Willis and W. R. Hingst, *Flowfield Measurements in a Slot-Bled Oblique Shock-Wave and Turbulent Boundary-Layer Interaction*, AIAA Paper 1995, 0032.

[28] A. Hamed, J. J. Yeuan and Y. D. Jun, *Flow Characteristics in Boundary-Layer Bleed Slots with Plenum*, AIAA Paper 1995, 0033.

[29] B. P. Willis and D. O. Davis, *Boundary Layer Development Downstream of a Bleed Mass Flow Removal Region*, AIAA Paper 1996, 3278.

[30] M. Mani, A. Cary and S. Ramakrishnan, *A Structured and Hybrid-Unstructured Grid Euler and Navier-Stokes Solver for General Geometry*, AIAA Paper 2004, 0524.

[31] A. Hamed, D. Basu and K. Das, Assessment of Hybrid Turbulence Models for Prediction of Unsteady High Speed Flow, *Computers and Fluids,* Vol. 26, 2007, pp 924-934.

[32] A. Hamed and C. Vogiatzis, Overexpanded Two-Dimensional Convergent-Divergent Nozzle Performance: Effects of Three Dimensional Flow Interactions, *Journal of Propulsion and Power*, Vol. 14, No. 2, pp. 234-240, March-April 1998.

[33] A. Hamed and A. Mohamed, *Assessment of Shock Induced Flow Separation and Shear Layer Mixing Predictions in Nozzles and High Speed Jet*, AIAA Paper 2001, 0225.

[34] M. Schoenenberger, I. Greber and D. O. Davis, *Flow Measurements Downstream of a Single Bleed Hole in a Subsonic, Turbulent Boundary Layer Using a New 5-Hole Pressure Probe*, AIAA Paper 1999, 0293.